

Fabrication of Graphene Oxide/Zinc Oxide Hybrid Nanocomposite and Assessment on Structural, Thermal and Optical Characterizations

SANOOP PADINHATTAYIL and K. SHESHAPPA RAI*

Department of Post-Graduate Studies and Research in Polymer Science, University of Mysore, Sir M. Visvesvaraya Post-Graduate Centre, Tubinakere, Mandya-571402, India

*Corresponding author: E-mail: sheshapparai19@gmail.com

Received: 5 October 2019;

Accepted: 30 November 2019;

Published online: 25 February 2020;

AJC-19807

The present work provides a selective review of research activities that focus on the graphene oxide (GO) and zinc oxide (ZnO) hybrid nanomaterials and their physical characterizations. The graphene oxide nanoparticle was prepared by modified Hummer's method and the nanohybrids of GO/ZnO prepared by chemical method. Nanohybrids were characterized by thermogravimetric analyzer to find the thermal stability of the hybrid material, the structural nature and crystal size by P-XRD, functional group identification and surface morphology by using FTIR & SEM technique. This method provides a facile method to synthesize the nanohybrid and will be freely extended to do the research on other class of hybrids based of graphene oxide.

Keywords: Hybrid nanocomposites, ZnO, Graphene oxide.

INTRODUCTION

Nanotechnology is an interdisciplinary innovation that has been blasting in numerous zones including electronics, materials science, mechanics, optics and biotechnology [1]. Manufacturing nanomaterials, for example nanoparticles, nanotubes, clusters, nanowires, nanorods and thin film is the key part for fruitful improvement of nanotechnology because of their concoction and physical properties result from the nano size impact [2,3]. Nanocomposites are composites in which at any rate one of the phases shows measurements in the nanometre scale [4]. The solitary properties and broad range of applications in diverse areas makes the nanocomposites distinctive [5-8]. Novel properties of nanocomposites could be obtained by the joined characteristics of parent constituents in a single material. One dimensional nanoparticle is anticipating the relevant part of preparing the nano scale devices and nanocomposites [9]. The developing interest of new materials with customized physico-chemical properties has pushed hybrid materials to a place of noticeable quality in materials science by ethicalness of their exceptional new properties and multifunctional nature. Hybrid nanomaterials, shaped by at least two parts associated at the nanometer scale,

consolidate the inborn attributes of its individual constituents to extra properties because of synergistic impacts between the segments [10,11]. Therefore, the properties of hybrid nanomaterials can be tuned by changing their composition and morphology, prompting materials with upgraded execution attributes, for example, high thermal stability, mechanical strength, light discharge, gas penetrability, electron conductivity and controlled wetting highlights [12,13]. Inferable from their wide range of available properties, hybrid materials are rising stages for applications in amazingly differing fields, for example, optics, microelectronics, smart coatings, health and diagnostics, photovoltaic, fuel cells, pollution remediation, catalysis and sensors [14-17].

The carbon materials specifically graphene and graphene oxide (GO) have expressive interest in the research area from last half decade. Graphene oxide contains a bunch of receptive oxygen functional groups, which make it a solid chosen one for use in numerous applications through chemical functionalization. Graphene oxide is developed from graphite oxide and it has been a positive section for creating a huge scale generation of graphene [18-20]. Graphene, be that as it may, has significant drawback low dispersibility in water, making its surface zone decline and along these lines, constrains its

application. This is because of aggregation that is brought about by the solid van der Waals interactions and π - π stacking of the graphene sheets [21]. Intrigue has been focused on absorbing GO with different materials by hybridizing it with water-dispersibility materials [22]. Also, controlled oxidation gives tunability of the electronic and mechanical properties, including the probability of getting to zero-band gap graphene by means of a total expulsion of the C-O bonds [23]. Different functionalities on the outside of GO make it a perfect stage for concoction alteration, which may produce materials with astounding properties. Considering the rare electronic, thermal, mechanical and optical properties of GO leads to nano electronics, conductive films, super capacitors, nano sensors *etc.* applications [24-26]. Graphene oxide is accepting expanding consideration since it has the comparable properties to graphene just as the exceptional surface structures with the presented hydroxyl and carboxyl groups for the combination of GO-containing nanocomposites [27]. Various metal oxide inorganic nanoparticles like ZnO are used to hybridize with GO to get optoelectronic materials, electrode materials, antibacterial materials and photo catalytic materials [28-37].

Zinc oxide is a promising nano material for the acknowledgement and eventual fate of nanotechnology. Zinc oxide is a potential group II-VI semiconductor with unique optical and electrical properties. It's used in different applications like optoelectronics, gas sensors, energy storage and solar cells [38-40]. It is a non-harmful material, ecofriendly and has low generation cost [41]. In the previous two decades, the gigantic enthusiasm for ZnO is incited by its multifunctional character, which can be shifted by controlling the morphology and crystallinity zinc oxides' driving qualities are a wide band gap at 3.37 eV and an enormous exciton binding energy of 60 meV at room temperature [42]. These properties make a ZnO a promising semiconductor competitor with potential applications in light discharging diodes [9], dye-sensitized solar cells [43] and transparent electrodes [44]. Additionally, gas-detecting properties of nanostructured ZnO were effectively found [45,46]. Assessing the fantastic properties of ZnO and graphene oxide, its nanocomposite can empower adaptable properties with skill a long ways past those of the individual individuals.

In this paper, we report the synthesis and study of GO-ZnO hybrid nanocomposites were zinc acetate dihydrate was used as the precursor for this method. The X-ray diffraction, scanning electron microscopy, ultraviolet and thermogravimetric analysis characterization of the material was done to measure the structural, optical band gap and thermal degradation with respect to GO and ZnO.

EXPERIMENTAL

Graphite flake with particle size 60 meshes were obtained from Loba Chemie. Zinc acetate dihydrate, sulfuric acid, hydrochloric acid, ethanol hydrogen peroxide, potassium permanganate, sodium nitrate, were purchased from Central Drug House, New Delhi, India and double distilled water was used for the experiments.

Preparation of graphene oxide: Graphene oxide was prepared using modified Hummers method [47]. Commonly, 5 g of graphite flakes was added to 120 mL of concentrated

H₂SO₄ and mixed uniformly by maintaining temperature below 5 °C. To the above solution mixture slowly added 20 g of KMnO₄ and then stirred for 1 h with same condition. Afterward add 2.5 g of NaNO₃ with a maximum temperature of 15 °C. The reaction was stirred at 35 °C for 6 h and to the resulting solution adds excess water for dilution. Add 30 % H₂O₂ to the reaction mass to ensure the completion reaction of KMnO₄. After 15 min of stirring the solution mixture was centrifuged followed by several washes with dilute HCl (5 %) and water to reach the pH value 7. The resulted product was dried at 60 °C in an air oven to obtain the pure GO.

Synthesis of GO/ZnO hybrid nanocomposites: The GO/ZnO hybrid nanocomposite was synthesized by simple wet chemical method [48]. In this method, graphene oxide was dispersed in ethanol (2:1 wt/vol ratio) and the solution mixture was sonicated for 1 h at room temperature. Afterward Zn(CH₃COO)₂·2H₂O (0.880 g) was dissolved in to the mixer. The pH of the solution was adjusted to 10 by adding 1 M NaOH solution and stirred for 30 min. The mixture was refluxed at 140 °C under inert atmosphere for 24 h. The prepared hybrid nanocomposites were centrifuged and washed with ethanol and distilled water for several times. Product was dried under vacuum oven for 6 h to get fine powder of GO/ZnO hybrid nanocomposites.

Characterization methods: XRD of GO and GO/ZnO hybrid were evaluated by using a XPERT-MPD diffractometre with CuK_α radiation with a 2 θ scanning range of 5-80° with slow scan rate of 0.02 %/s to point out the structure and average crystal size. The chemical compositions of the nanomaterials were point out from Fourier transform infrared spectroscopy. The thermal acts of the samples were investigated by a TGA analyzer at a heating rate of 10 °C/min and a temperature variation from 25 to 800 °C under inert atmosphere. The surface topology of the GO and GO/ZnO was evaluated by using SEM. The optical characterization of the nanomaterials is implicated by the UV-visible analysis.

RESULTS AND DISCUSSION

The XRD analysis were used to explore the compositions of the GO, ZnO and GO-ZnO nanocomposites (Fig. 1). The peaks listed at 50.31° and 71.56° imply the crystalline structure of graphite. The discernable peak of graphite at 26.47° shows that graphite is a highly oriented carbon material. The oxygen resonant groups on the GO surface could be appeared at 10.6° peak and the intensity of the peak was drastically decreased in hybrid nanocomposites [49]. The changes in the GO peaks indicate the exfoliation of GO because the deposition of ZnO nanoparticles. The major diffraction peaks are present between 20° and 70° (2 θ) reasons to the hexagonal ZnO crystal structure.

A fortuitous result of diffraction peaks for ZnO nanoparticles and ZnO/GO nanocomposite is profoundly amazing demonstrating the development of well crystalline structure of ZnO nanoparticles onto the GO surface.

From Table-1, GO has the average crystal size of 35.20 nm, ZnO has 26.24 and the GO/ZnO hybrid material has 50.94 nm. The average crystal size of the nanomaterials can be explain by using the Scherrer's formula:

$$D_p = K\lambda / (B \cos \theta)$$

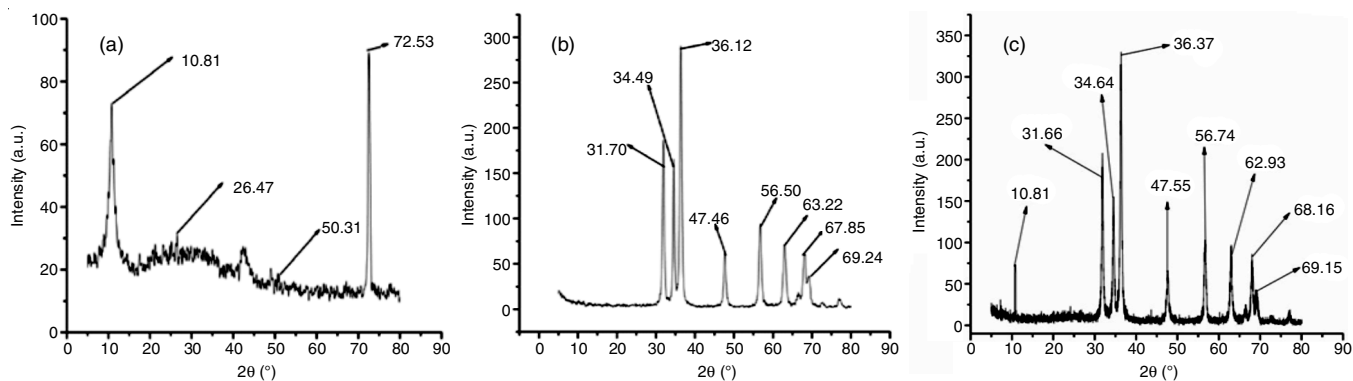


Fig. 1. XRD patterns of (a) GO; (b) ZnO and (c) GO/ZnO

TABLE-1 CRYSTAL SIZE CALCULATION OF GO, ZnO AND GO/ZnO NANOCOMPOSITE BY SCHERRER'S FORMULA			
Peak position $2\theta^a$ (°)	FWHM ^b B_{size} (°)	Dp^c (nm)	Dp average (nm)
GO			
9.9461	0.5280	15.79	35.20
26.5033	0.6298	13.55	
42.5308	0.6298	14.15	
77.6461	0.7680	13.88	
77.8900	0.0900	118.63	
ZnO			
31.8544	0.1574	54.86	26.74
34.5936	0.3149	27.62	
36.4799	0.3542	24.68	
47.5322	0.2362	38.41	
56.8160	0.2362	39.97	
62.9543	0.6298	15.46	
66.5768	0.6298	15.77	
68.2640	0.5510	18.21	
69.3017	0.4723	21.37	
77.0026	0.9600	11.05	
GO/ZnO nanocomposite			
9.6439	0.4079	20.43	50.94
26.3625	0.6298	13.54	
31.8362	0.3936	21.94	
34.4618	0.2362	36.81	
36.2436	0.1968	44.40	
42.9699	0.0580	153.86	
47.5900	0.0900	100.84	
56.6590	0.7872	11.98	
62.8258	0.4723	20.60	
68.0088	0.5760	17.39	
77.7500	0.0900	118.51	

^aXRD peak position, one half of 2θ ; ^bFull width at half maximum; ^cAverage crystal size (nm)

where, D_p = average crystallite size (nm) K = Scherrer's constant (K varies from 0.68 to 2.08. $K = 0.94$ for spherical crystallites with cubic symmetry), λ = X-ray wavelength. For mini XRD, B -FWHM (full width at half maximum) of XRD peak θ = XRD peak position, one half of 2θ .

The morphological characterizations of the synthesized GO, ZnO and ZnO/GO nanocomposite were examined by SEM and EDS.

Fig. 2a shows the basic shape of GO sheet that was significantly exfoliated and looks like pieces of crystals with a dimension ranging from several hundred nm to several microns. Fig. 2b shows the view of ZnO/GO nanocomposite, which indicates that ZnO nanoparticles are closely anchored at the surface of GO. The development of nanoparticles agglomerated fit as different size and direction might be ascribed because of the uncontrolled nucleation development during the testimony of ZnO nanoparticles in the GO matrix. From Fig. 3 deep-rooted the formation of ZnO shape and oxidation of exfoliated graphene oxide by energy dispersive spectroscopy (EDS) shows the energy dispersive absorption X-ray spectrum (EDAX) results of GO/ZnO nanocomposites. It is well-known that the EDS is a semi-quantitative micro chemical investigation technique and can be utilized to appraise the opus of blended structures. The presence of zinc, carbon and oxygen elements were affirmed from EDS.

FTIR spectra investigation was performed for the basic explanation and assessment of useful functional groups of the materials. In the Fig. 4a, 3430 cm^{-1} absorption band indicates the O-H group stretching vibrations of GO. The C=O stretching of carboxylic and carbonyl moiety functional groups are observed at 1627 cm^{-1} . The peaks at 1054.10 and 918.51 cm^{-1} are noted to the stretching of C-OH and C-O respectively. The

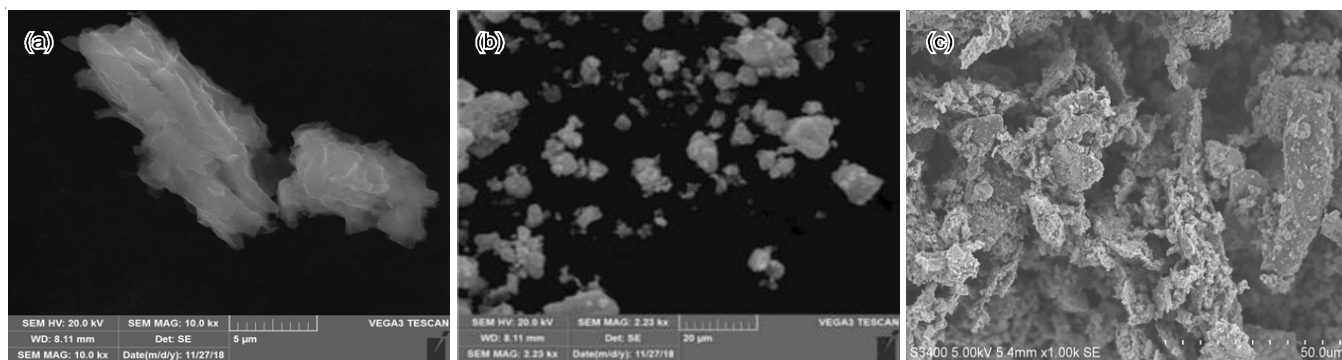


Fig. 2. SEM image of (a) GO; (b) ZnO and (c) GO/ZnO hybrid

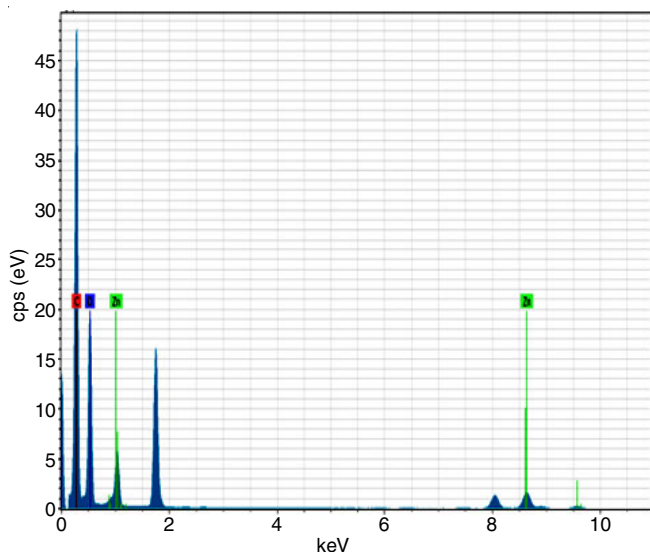


Fig. 3 EDS image of GO/ZnO hybrid

peaks around 2924 and 2855 cm^{-1} can be assigned to the asymmetric and symmetric vibrations of C-H.

On account of GO-ZnO composite, there is a significant decrease of GO and it diminished the oxygen functional groups in the composite materials (Fig. 4c). The absorbance peaks

at 1600 and 450 cm^{-1} means the drawn vibration of graphene oxide (C=C) and extending vibration of ZnO. In this way, these confirmations complete the arrangement of ZnO on GO matrix.

The material surface composition and its chemical states can be identified by means of XPS spectrum analysis according to the characterizing binding energies of the different elements on the material outfit. From Fig. 5a the doublet about 1022 and 1045 eV in the XPS spectra of Zn-2p core level regions meets the Zn-2p_{3/2} and 2p_{1/2} core levels [50]. The first peak is evident for the ZnO matrix with free of oxygen.

The C1s XPS spectra of GO from Fig. 5b contains three peaks at 284.6, 286.6 and 288.5 eV favours to the sp^2 carbon, the peroxide and the carboxyl functional groups, respectively [51].

Even the position of the lines is very similar in both C1s spectra, the intensity of the peaks corresponding to the oxygen functional groups is much reduced in case of the spectrum corresponding to ZnO/GO composite (Fig. 6) as compared with the GO sample. This feature confirms the partial reduction of the oxygen functional groups in the presence of ZnO nanoparticles.

The optical properties of the GO-ZnO nanocomposites were clarified with UV-visible spectroscopy. The UV range of GO-ZnO nano composite alongside the unadulterated GO and ZnO is shown in Fig. 7.

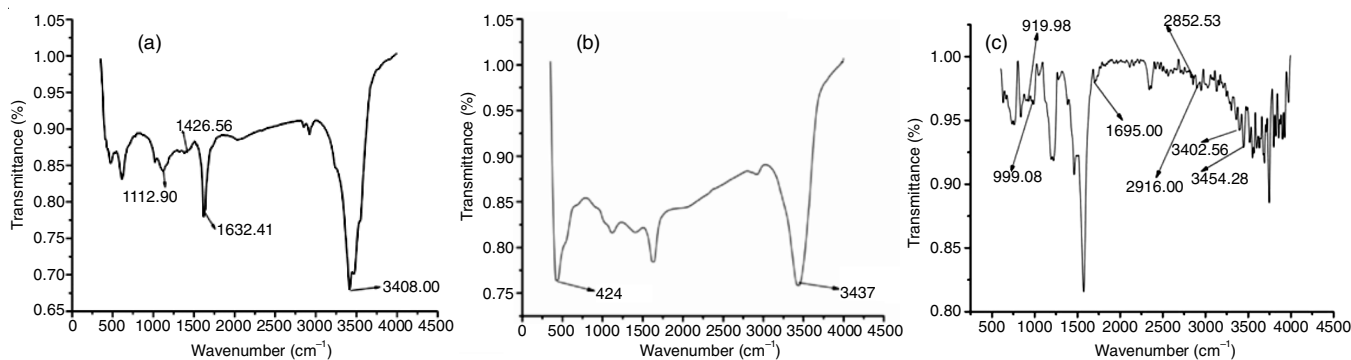


Fig. 4. FTIR spectra of (a) GO; (b) ZnO and (c) GO/ZnO hybrid

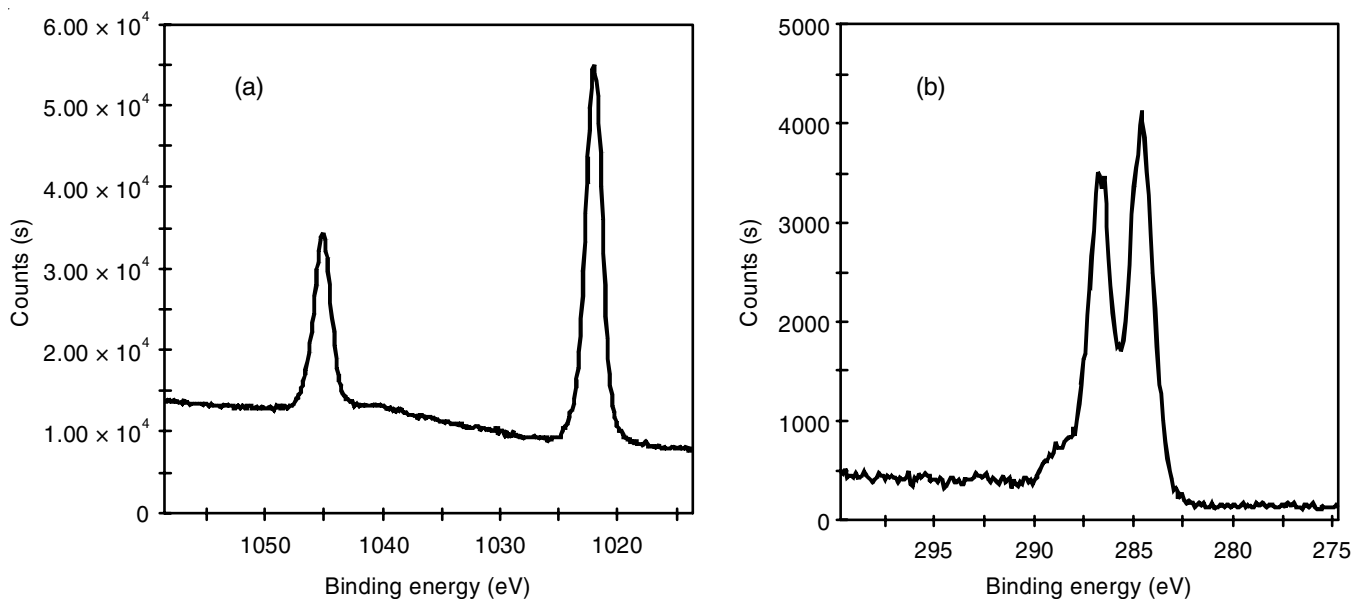


Fig. 5. XPS core level spectra (a) ZnO and (b) GO

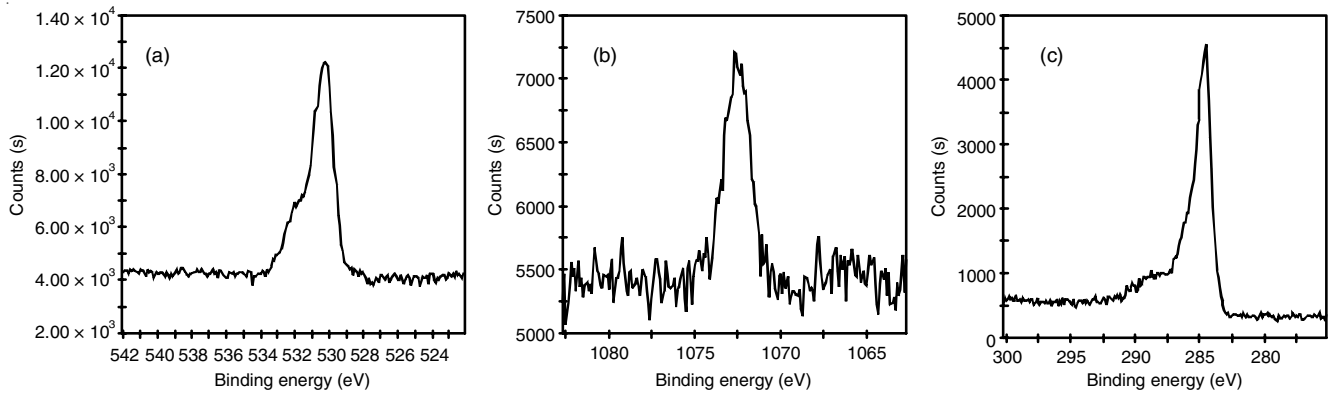


Fig. 6. XPS survey and core level spectra's GO/ZnO hybrid nanocomposite

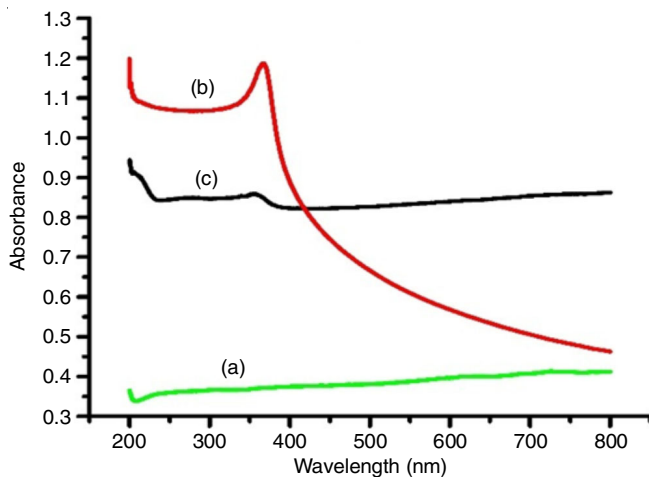


Fig. 7. UV absorption spectra of (a) GO, (b) ZnO and (c) GO/ZnO hybrid composite

The aromatic C-C bond of GO feature to the absorption at 334 nm in the $n-\pi^*$ transitions [52]. Where in, ZnO a wide retention peak is observed to be around 366 nm, which is quality of the Wurtzite hexagonal state ZnO, showing that the incorporated item is an unadulterated ZnO [53].

The energy gap of the pure GO, ZnO sample and the composites are estimated using Tauc plot and given in Table-2. The band gap of the GO was found to be 5.086 eV while that of ZnO was estimated to be 3.072 eV. The hybrid material is having Bandgap of 3.46 eV which is indication of the reduction of GO in the presence of ZnO.

The decomposition property of GO, ZnO and GO-ZnO hybrid nanocomposites has been examined by thermogravimetric analysis. Fig. 8a demonstrates the thermal nature of

Material	Energy gap (eV)
GO	3.71
ZnO	3.39
GO/ZnO hybrid	3.46

the GO, which is moderately great. However at about 200 °C, the thermal stability of GO was found to diminish, because of the decay of carboxylic and arrival of CO₂ gas.

The TGA diagram (Fig. 8b) of the ZnO nanoparticles was demonstrating that proceeds with weight reduction was occurred up to 600 °C, after that there is no critical loss of warmth was watched. At 250 °C onwards sharp weight reduction found. The thermal stability of GO/ZnO is drawn in Fig. 8c and it looks there is a gradual weight loss of the material and has a better thermal stability than the individuals. Weight (%) loss has happened up to 700 °C.

Conclusion

In present investigation ZnO nanoparticles and GO are incorporated by precipitation technique and Hummer's method individually. The structural composition of ZnO, GO and GO/ZnO hybrid nanocomposites have been explored. From the XRD results the size of ZnO nanoparticles were assessed as 26.20 nm, GO 35.20 nm and that of GO/ZnO hybrids 50.94 nm by the XRD Scherer's formula. From SEM characterization, the ZnO nanoparticles demonstrated a well-defined dispersion on to the surface of GO matrix. Also the EDS confirm the presence of elements in the core material from the GO and ZnO nanomaterials. Results of FT-IR and XPS showed that

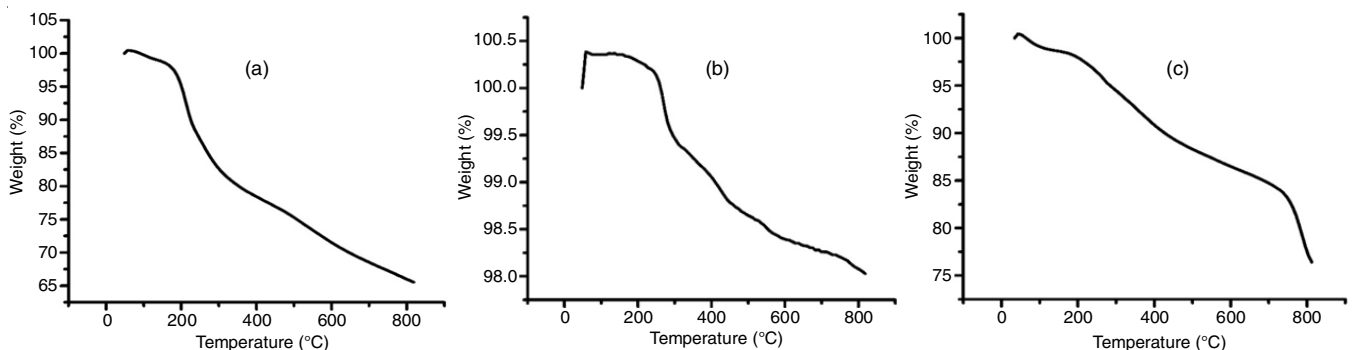


Fig. 8. Thermogravimetric analysis of (a) GO; (b) ZnO and (c) GO/ZnO hybrid

the nanocomposite was formed by the reaction between GO and ZnO. It was presumed that the nanocomposite structure decreased the band hole of GO nanoparticles. The thermal stability of GO/ZnO is more than that of the GO and ZnO nanoparticles.

CONFLICT OF INTEREST

The authors declare that there is no conflict of interests regarding the publication of this article.

REFERENCES

1. A.L. Porter and J. Youtie, *J. Nanopart. Res.*, **11**, 1023 (2009); <https://doi.org/10.1007/s11051-009-9607-0>
2. C.A. Charitidis, P. Georgiou, M.A. Koklioti, A.-F. Trompeta and V. Markakis, *Manufacturing Rev.*, **1**, 19 (2014); <https://doi.org/10.1051/mfreview/2014009>
3. J. Jeevanandam, A. Barhoum, Y.S. Chan, A. Dufresne and M.K. Danquah, *Beilstein J. Nanotechnol.*, **9**, 1050 (2018); <https://doi.org/10.3762/bjnano.9.98>
4. R. Roy, R.A. Roy and D.M. Roy, *Mater. Lett.*, **4**, 323 (1986); [https://doi.org/10.1016/0167-577X\(86\)90063-7](https://doi.org/10.1016/0167-577X(86)90063-7)
5. L.L. Be Creft and C.K. Ober, *Chem. Mater.*, **9** (1999).
6. P. Tang, H.-K. Chan and J.A. Raper, *Powder Technol.*, **147**, 64 (2004); <https://doi.org/10.1016/j.powtec.2004.09.036>
7. B.H. Kim, J.H. Jung, S.H. Hong, J.W. Kim, H.J. Choi and J. Joo, *Curr. Appl. Phys.*, **1**, 112 (2002); [https://doi.org/10.1016/S1567-1739\(00\)00021-3](https://doi.org/10.1016/S1567-1739(00)00021-3)
8. D.G. Yu and J.H. An, *Colloids Surf. A Physicochem. Eng. Asp.*, **237**, 87 (2004); <https://doi.org/10.1016/j.colsurfa.2004.02.009>
9. Y. Sun, Y. Yin, B.T. Mayers, T. Herricks and Y. Xia, *Chem. Mater.*, **14**, 4736 (2002); <https://doi.org/10.1021/cm020587b>
10. D.A. Loy and K.J. Shea, *Chem. Rev.*, **95**, 1431 (1995); <https://doi.org/10.1021/cr00037a013>
11. U. Díaz, D. Brunel and A. Corma, *Chem. Soc. Rev.*, **42**, 4083 (2013); <https://doi.org/10.1039/c2cs35385g>
12. R. Hayami, K. Wada, I. Nishikawa, T. Sagawa, K. Yamamoto, S. Tsukada and T. Gunji, *Polym. J.*, **49**, 665 (2017); <https://doi.org/10.1038/pj.2017.34>
13. G. Soliveri, R. Annunziata, S. Arduizzone, G. Cappelletti and D. Meroni, *J. Phys. Chem. C*, **116**, 26405 (2012); <https://doi.org/10.1021/jp309397c>
14. U. Diaz and A. Corma, *Chemistry*, **24**, 3944 (2018); <https://doi.org/10.1002/chem.201704185>
15. D. Meroni, S. Arduizzone, U.S. Schubert and S. Hoepfner, *Adv. Funct. Mater.*, **22**, 4376 (2012); <https://doi.org/10.1002/adfm.201200673>
16. C. Sanchez, P. Belleville, M. Popall and L. Nicole, *Chem. Soc. Rev.*, **40**, 696 (2011); <https://doi.org/10.1039/c0cs00136h>
17. A. Colombo, C. Dragonetti, M. Magni, D. Meroni, R. Ugo, G. Marotta, M. Grazia Lobello, P. Salvatori and F. De Angelis, *Dalton Trans.*, **44**, 11788 (2015); <https://doi.org/10.1039/C5DT01216C>
18. D.R. Dreyer, S. Park, C.W. Bielawski and R.S. Ruoff, *Chem. Soc. Rev.*, **39**, 228 (2010); <https://doi.org/10.1039/B917103G>
19. A. Safavi, M. Tohidi, F.A. Mahyari and H. Shahbaazi, *J. Mater. Chem.*, **22**, 3825 (2012); <https://doi.org/10.1039/c2jm13929d>
20. G. Wang, B. Wang, J. Park, Y. Wang, B. Sun and J. Yao, *Carbon*, **47**, 3242 (2009); <https://doi.org/10.1016/j.carbon.2009.07.040>
21. X. Huang, Z. Yin, S. Wu, X. Qi, Q. He, Q. Zhang, Q. Yan, F. Boey and H. Zhang, *Small*, **7**, 1876 (2011); <https://doi.org/10.1002/sml.2011002009>
22. J. Liu, G. Liu and W. Liu, *Chem. Eng.*, **257**, 299 (2014); <https://doi.org/10.1016/j.cej.2014.07.021>
23. K.A. Mkhoyan, A.W. Contryman, J. Silcox, D.A. Stewart, G. Eda, C. Mattevi, S. Miller and M. Chhowalla, *Nano Lett.*, **9**, 1058 (2009); <https://doi.org/10.1021/nl8034256>
24. Y.W. Wang, A. Cao, Y. Jiang, X. Zhang, J.H. Liu, Y. Liu and H. Wang, *ACS Appl. Mater. Interf.*, **6**, 2791 (2014); <https://doi.org/10.1021/am4053317>
25. S. Liu, T.H. Zeng, M. Hofmann, E. Burcombe, J. Wei, R. Jiang, J. Kong and Y. Chen, *ACS Nano*, **5**, 6971 (2011); <https://doi.org/10.1021/nn202451x>
26. D.R. Dreyer, S. Park, C.W. Bielawski and R.S. Ruoff, *Chem. Soc. Rev.*, **39**, 228 (2010); <https://doi.org/10.1039/B917103G>
27. B. Li, T. Liu, Y. Wang and Z. Wang, *J. Colloid Interface Sci.*, **377**, 114 (2012); <https://doi.org/10.1016/j.jcis.2012.03.060>
28. T.A. Pham, B.C. Choi, K.T. Lim and Y.T. Jeong, *Appl. Surf. Sci.*, **257**, 3350 (2011); <https://doi.org/10.1016/j.apsusc.2010.11.023>
29. G. Williams, B. Seger and P.V. Kamat, *ACS Nano*, **2**, 1487 (2008); <https://doi.org/10.1021/nn800251f>
30. P.V. Kamat, *J. Phys. Chem. Lett.*, **1**, 520 (2010); <https://doi.org/10.1021/jz900265j>
31. X.Y. Yang, X.Y. Zhang, Y.F. Ma, Y. Huang, Y.S. Wang and Y.S. Chen, *J. Mater. Chem.*, **19**, 2710 (2009); <https://doi.org/10.1039/b821416f>
32. S.M. Paek, E. Yoo and I. Honma, *Nano Lett.*, **9**, 72 (2009); <https://doi.org/10.1021/nl802484w>
33. I.V. Lightcap, T.H. Kosel and P.V. Kamat, *Nano Lett.*, **10**, 577 (2010); <https://doi.org/10.1021/nl9035109>
34. J.F. Shen, M. Shi, N. Li, B. Yan, H.W. Ma, Y.Z. Hu and M.X. Ye, *Nano Res.*, **3**, 339 (2010); <https://doi.org/10.1007/s12274-010-1037-x>
35. J. Li and C.Y. Liu, *Eur. J. Inorg. Chem.*, **8**, 1244 (2010); <https://doi.org/10.1002/ejic.200901048>
36. G. Williams and P.V. Kamat, *Langmuir*, **25**, 13869 (2009); <https://doi.org/10.1021/la900905h>
37. O. Akhavan, *Carbon*, **49**, 11 (2011); <https://doi.org/10.1016/j.carbon.2010.08.030>
38. A.B. Djuricic, A.M.C. Ng and X.Y. Chen, *Prog. Quantum Electron.*, **34**, 191 (2010); <https://doi.org/10.1016/j.pquantelec.2010.04.001>
39. G. Singh, A. Choudhary, D. Haranath, A.G. Joshi, N. Singh, S. Singh and R. Pasricha, *Carbon*, **50**, 385 (2012); <https://doi.org/10.1016/j.carbon.2011.08.050>
40. K.K. Purushothaman, V. Suba Priya, S. Nagamuthu, S. Vijayakumar and G. Muralidharan, *Micro & Nano Lett.*, **6**, 668 (2011); <https://doi.org/10.1049/mnl.2011.0260>
41. H. Jiang, J.Q. Hu, F. Gu and C.Z. Li, *J. Phys. Chem. C*, **112**, 12138 (2008); <https://doi.org/10.1021/jp802423z>
42. H.G. Guo, J.Z. Zhou and Z.G. Lin, *Electrochem. Commun.*, **10**, 146 (2008); <https://doi.org/10.1016/j.elecom.2007.11.010>
43. Q.F. Zhang, C.S. Dandeneau, X.Y. Zhou and G.Z. Cao, *Adv. Mater.*, **21**, 4087 (2009); <https://doi.org/10.1002/adma.200803827>
44. M.F. Melendrez, K. Hanks, F. Leonard-Deepak, F. Solispomar, E. Martinez-Guerra, E. Perez-Tijerina and M. Joseyacaman, *J. Mater. Sci.*, **47**, 2025 (2012); <https://doi.org/10.1007/s10853-011-6002-x>
45. M. Chen, Z.H. Wang, D.M.G.U. Han, F. Gu and G. Guo, *Sens. Actuators B Chem.*, **157**, 565 (2011); <https://doi.org/10.1016/j.snb.2011.05.023>
46. G.K. Mani and J.B.B. Rayappan, *Sens. Actuators B Chem.*, **183**, 459 (2013); <https://doi.org/10.1016/j.snb.2013.03.132>
47. W.S. Hummers Jr. and R.E. Offeman, *J. Am. Chem. Soc.*, **80**, 1339 (1958); <https://doi.org/10.1021/ja01539a017>
48. Y. Bu, Z. Chen, W. Li and B. Hou, *ACS Appl. Mater. Interfaces*, **5**, 12361 (2013); <https://doi.org/10.1021/am403149g>
49. Y. Li, W. Gao, L. Ci, C. Wang and P.M. Ajayan, *Carbon*, **48**, 1124 (2010); <https://doi.org/10.1016/j.carbon.2009.11.034>
50. O. Lupan, G.A. Emelchenko, V.V. Ursaki, G. Chai, A.N. Redkin, A.N. Gruzintsev, I.M. Tiginyanu, L. Chow, L.K. Ono, B. Roldan Cuenya, H. Heinrich and E.E. Yakimov, *Mater. Res. Bull.*, **45**, 1026 (2010); <https://doi.org/10.1016/j.materresbull.2010.03.027>
51. S. Park, J. An, I. Jung, R.D. Piner, S.J. An, X. Li, A. Velamakanni and R.S. Ruoff, *Nano Lett.*, **9**, 1593 (2009); <https://doi.org/10.1021/nl803798y>
52. A. Shokry, M.M.A. Khalil, H. Ibrahim, M. Soliman and S. Ebrahim, *Sci. Rep.*, **9**, 16984 (2019); <https://doi.org/10.1038/s41598-019-53584-6>
53. N. Preda, M. Enculescu, C. Florica, A. Costas, A. Evangelidis, E. Matei and I. Enculescu, *Dig. J. Nanomater. Biostruct.*, **8**, 1591 (2013).